Biophysical Journal, Volume *118*

Supplemental Information

Membrane Protein Dimerization in Cell-Derived Lipid Membranes Measured by FRET with MC Simulations

Jan Škerle, Jana Humpolíčková, Nicholas Johnson, Petra Rampírová, Edita Poláchová, Monika Fliegl, Jan Dohnálek, Anna Suchánková, David Jakubec, and Kvido Strisovsky

Fig. S1: Illustration of individual steps during the bleedthrough removal.

(A) Temporal evolution of fluorescence intensity of eGFP (green) and the mixed fluorescence signal of mCherry and bleed through from the eGFP channel (black); (**B)** TCSPC histogram of the mixed signal (black), eGFP (green) in the mCherry channel, and mCherry excited by the cw laser (red); (**C)** Mathematical filters for the mCherry signal (red) and for the eGFP signal in the mCherry channel (green); (**D)** Filtered autocorrelation functions of eGFP (green), mCherry (red), and the crosscorrelation function of the eGFP and mCherry signal (red-green).

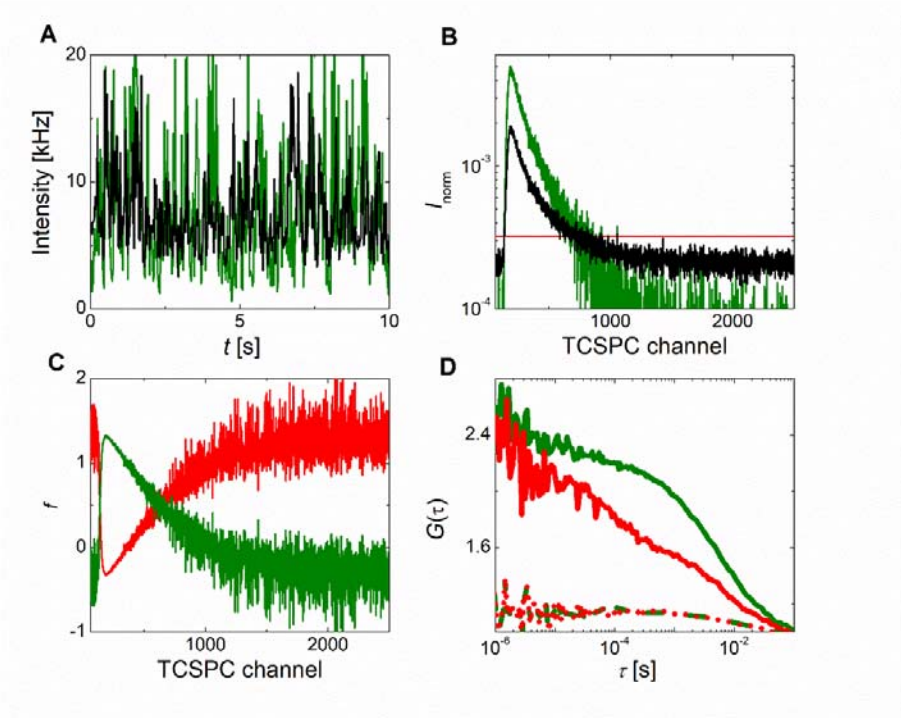

Channel bleed-through removal

Our microscopy setup does not allow for pulsed interleaved excitation (PIE), i.e. alternating, nanosecond-scaled pulsing of two lasers, we have employed strategy based on fluorescence lifetime correlation spectroscopy (FLCS) to remove the bleed- through signal. PIE can be automatically used for removal of the GFP signal that falls into the mCherry detection channel as the photons arising upon the blue excitation pulse arrive at different time range than those that were generated by the green laser. If this is not feasible, a similar effect can be achieved by combining of the pulsed and continuous wave (cw) excitation. The signal in the mCherry channel $I_j^{\text{mCherry}}(t)$ is mixed from the real mCherry contribution $w^{\text{mCherry\_561}}(t)$, that

has been excited by the cw 561nm laser line, and from the GFP contribution $w^{\mathrm{GFP\_490}}(t)$ that has been generated by the pulsed 490nm laser line:

$$I_j^{\mathrm{mCherry}}(t) = w^{\mathrm{mCherry\_561}}(t) \cdot p_j^{\mathrm{flat}} + w^{\mathrm{GFP\_490}}(t) \cdot p_j^{\mathrm{exponential}}.$$

(1)

While TCSPC profile of the first contribution is flat p_j^{flat}, the profile of the latter is exponential $p_j^{\mathrm{exponential}}$. j stands for the j^{th} TCSPC channel. FLCS suggests construction of mathematical filters, orthogonal to the two TCSPC profiles, that can be used to calculate intensity contribution at given time t of the one or the other signal contributor:

$$f_j^k = \left(\left[\boldsymbol{M}^T \mathrm{diag}\langle I_j^{\mathrm{mCherry}}(t) \rangle_t^{-1} \cdot \boldsymbol{M} \right]^{-1} \cdot \boldsymbol{M}^T \cdot \mathrm{diag}\langle I_j^{\mathrm{mCherry}}(t) \rangle_t^{-1} \right)_{kj},$$

(2)

Where k stays either for the flat contribution of 561nm excitation, or for the exponential 490nm excitation. $\boldsymbol{M}$ is the matrix consisting of the TCSPC profiles:

$$\boldsymbol{M}_{jk} = p_j^k.$$

(3)

Finally, the autocorrelation function of the mCherry signal G^{mCherry} and its crosscorrelation function G^{cc} with the GFP signal are calculated as follows:

$$G^{\mathrm{mCherry}}(\tau) = \frac{\sum_{i=1}^{N} \sum_{j=1}^{N} f_i^{mCherry\_561} f_j^{\mathrm{mCherry\_561}} \langle I_i^{\mathrm{mCherry}}(t) I_i^{\mathrm{mCherry}}(t+\tau) \rangle_t}{\sum_{i=1}^{N} \sum_{j=1}^{N} f_i^{mCherry\_561} f_j^{\mathrm{mCherry\_561}} \langle I_i^{\mathrm{mCherry}}(t) \rangle_t \langle I_j^{\mathrm{mCherry}}(t) \rangle_t},$$

(4)

$$G^{\mathrm{cc}}(\tau) = \frac{\sum_{i=1}^{N} f_i^{\mathrm{mCherry\_561}} \langle I_i^{\mathrm{mCherry}}(t) I^{GFP}(t+\tau) \rangle_t}{\sum_{i=1}^{N} f_i^{\mathrm{mCherry\_561}} \langle I_i^{\mathrm{mCherry}}(t) \rangle_t \langle I^{GFP}(t) \rangle_t}.$$

(5)

The illustrative decays and corresponding filters are shown above.

Fig. S2: Illustrative step-by-step description of the MC simulation approach

(A) Random distribution of protein monomers and dimers within the simulated area. Proteins are assigned donors (blue)/acceptors (yellow). (**B-D)** Time that elapses since the donor has been excited until it transfers its energy to an acceptor, shown on three random excitations. **(E)** Cumulative histogram of the excited state durations. Black curve sums the excitations in panels **B**, **C** and **D**; red curve results from large number of random excitations. (**F)** The probability that the donor is in the excited state (yellow curve) is a product of the probability that the energy is not transferred by FRET (red curve) and the probability that the energy is released by fluorescence or by a different non-radiative pathway (green curve). (**G**) The final donor excited state lifetime histogram (dash-dotted curve) is convolved with experimentally measured instrument response function (black curve). The resulting function (yellow solid curve) can be compared with the experimental data.

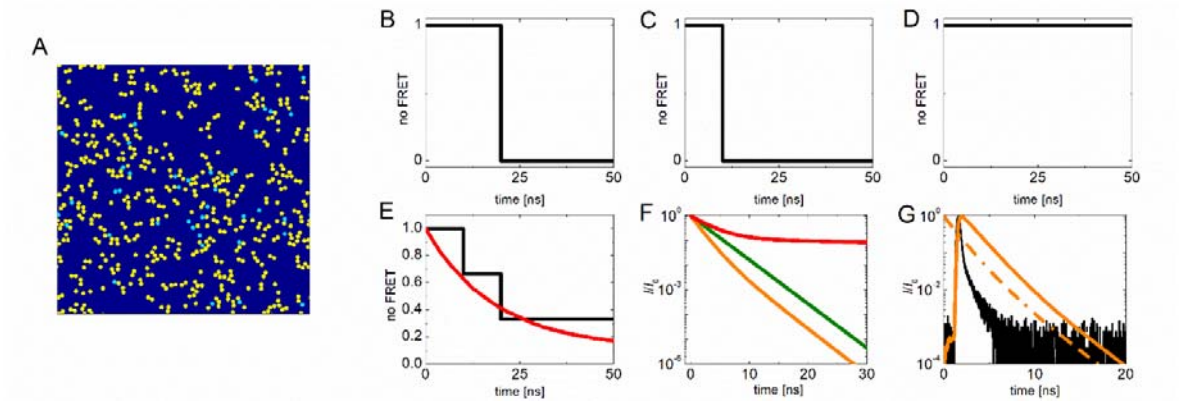

Fig. S3: GFP and mCherry fusions to human RHBDL2 are enzymatically active in cells.

Plasmids encoding human RHBDL2 fused to the HA tag, eGFP or mCherry at the N-terminus were transfected into HEK293ET cells alone or together with plasmid encoding RHBDL2 substrate Spint-1 tagged by a Strep tag (16). Cell lysates and media were collected for analysis as described (16). Asterisk (*) marks a non-specific band.

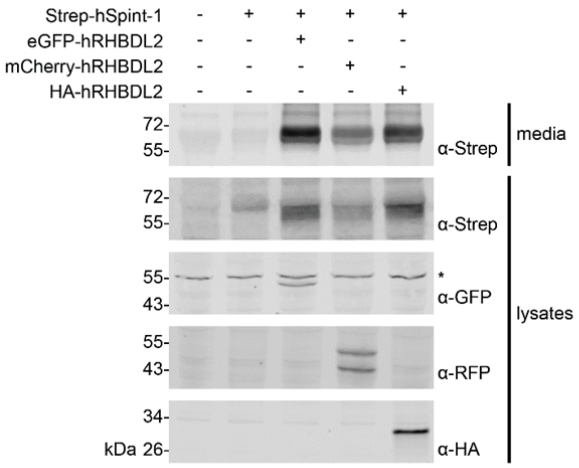

Fig. S4: Dimer fractions obtained from the auto- and crosscorrelation amplitudes.
The error bars represent the standard error of the mean.

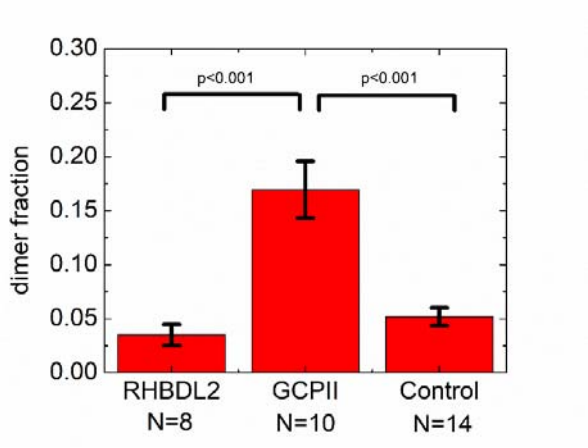

The dimer fraction was estimated from the autocorrelation amplitudes of eGFP and mCherry and from the crosscorrelation amplitude (G, R, cc). In the estimation we assume that the blue (for eGFP) and green (for mCherry) focal volume as well as the overlap of the two foci are equal, the amplitudes are related to the number of eGFP-/mCherry- labelled proteins as follows:

$$G = \frac{g+rg+4*gg}{(g+rg+2gg)^2}, \qquad R = \frac{r+rg+4*rr}{(r+rg+2rr)^2}, \qquad cc = \frac{rg}{(r+rg+2rr)(g+rg+2gg)}.$$

(6)

r, *g*, *rr*, *gg*, and *rg* stay for numbers of mCherry-/eGFP- labeled monomer, mCherry-/eGFP-homodouble- labelled dimer and number of heterodouble- labelled dimer in the focal volume, respectivelly.

The probabilities of homo- and hetero- labelling of the dimer p_{gg}, p_{rr}, and p_{rg} obey the binomial distribution:

$$p_{gg} = \frac{(g+2gg+rg)^2}{(g+r+2gg+2rr+rg)^2},\ p_{rr} = \frac{(r+2rr+rg)^2}{(g+r+2gg+2rr+rg)^2}, p_{rg} = \frac{2*(r+rr+rg)(g+gg+rg)}{(r+g+2rr+2gg+rg)^2}.$$

(7)

We assumed that the homodouble- labelled protein fraction is negligible (protein concentration is below K_D), the dimer fraction Fr_D can be calculated according to the formula:

$$Fr_D = \frac{cc(R+G)^2}{cc(R^2+G^2)+G+R}.$$

(8)

The assumption that the contribution of *gg* and *rr* to the ACF amplitudes was verified by back-calculation of the amplitudes from the calculated concentrations according to the correct formulas.

Fig. S5: Comparison of lateral concentration of acceptors obtained by fitting of the donor fluorescence decay by Baumann-Fayer model and obtained from the FCS extrapolation approach suggested by us.

The experiment was performed in GUVs with ATTO488-DOPE as a donor and with ATTO647N-DOPE as acceptor.

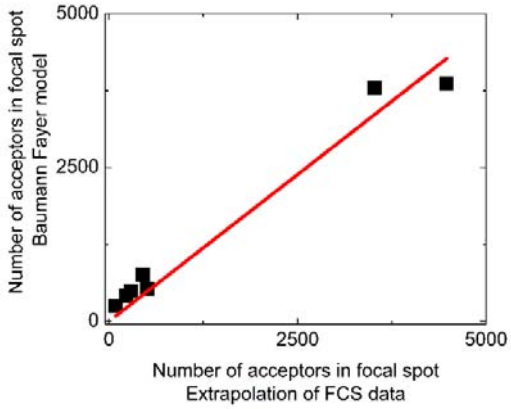

Fig. S6: Comparison of acceptor dependent FRET efficiencies for eGFP/mCherry pair attached to the membrane of GUVs by different linker.

NiNTA spiked GUVs were decorated by His-tagged eGFP/mCherry at increasing concentration of acceptors and the FRET efficiency was evaluated. The linker between the tag and the fluorescent protein was formed either by 18 amino acid residues (black squares) or by the 72 amino acid N-terminal cytosolic domain of RHBDL2 (R2Ncyto) (red circles).

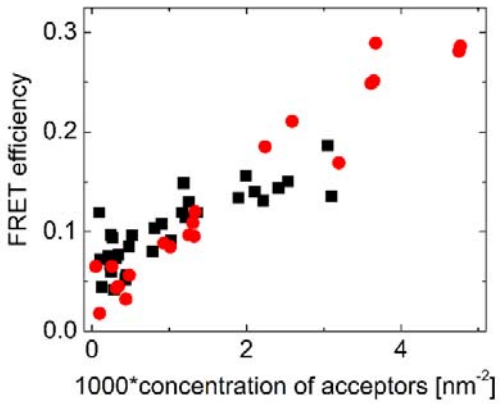

Fig. S7: Comparison of expression levels of transfected eGFP/mCherry-RHBDL2 to the levels of endogenous RHBDL2

Approximately equal amounts of cell lysates of HeLa cells transiently transfected by eGFP/mCherry-RHBDL2 and human keratinocytes HaCaT with or without expressed shRNA targeting endogenous RHBDL2 were separated by SDS PAGE and analyzed by quantitative immunoblotting using α-RHBDL2 primary antibody and fluorescent secondary antibody as described in Methods. Fluorescence of the secondary antibody was visualized using infrared scanner, and expression levels of RHBDL2 were quantified from the integrated fluorescence intensity values summed up for the specific bands (marked by black triangles) and normalized for the total protein in each lane indicated by the fluorescence intensity of the Revert staining (Methods).

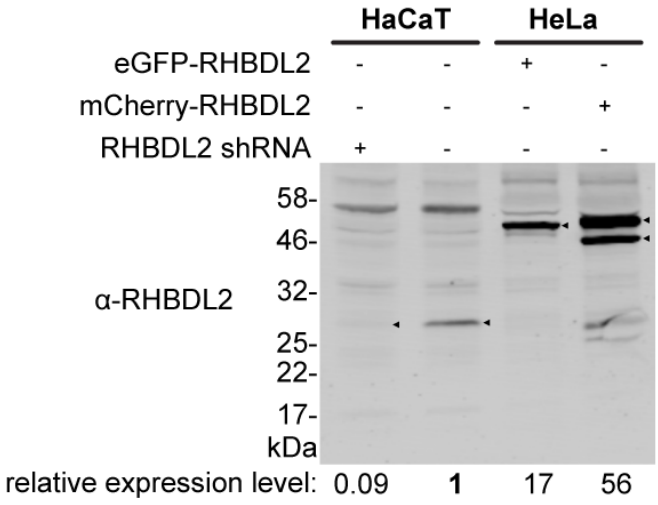

Fig. S8: Some additional cells observed in the relocalization experiment shown in Fig. 6.

Fluorescent constructs of human RHBDL2 fused to either eGFP or mCherry with or without the ER-retaining KDEL signal fused to the very C-terminus of each protein were co-expressed in HeLa cells, and live cell fluorescence was recorded 20-24 hrs after transfection. **A**, eGFP-RHBDL2 co-expressed with mCherry-RHBDL2; **B**, eGFP-RHBDL2-KDEL co-expressed with mCherry-RHBDL2-KDEL; **C**, eGFP-RHBDL2 co-expressed with mCherry-RHBDL2-KDEL. Note that while both fusions show strong plasma membrane localization including filopodia (A), KDEL tagging effectively relocalizes both fusions to the ER (B), while KDEL tagging of only one of the fusion proteins does not relocalize the other co-expressed one (C), meaning that the two fusion proteins do not stably interact with one another within the cell. Scale bars are 5 µm.

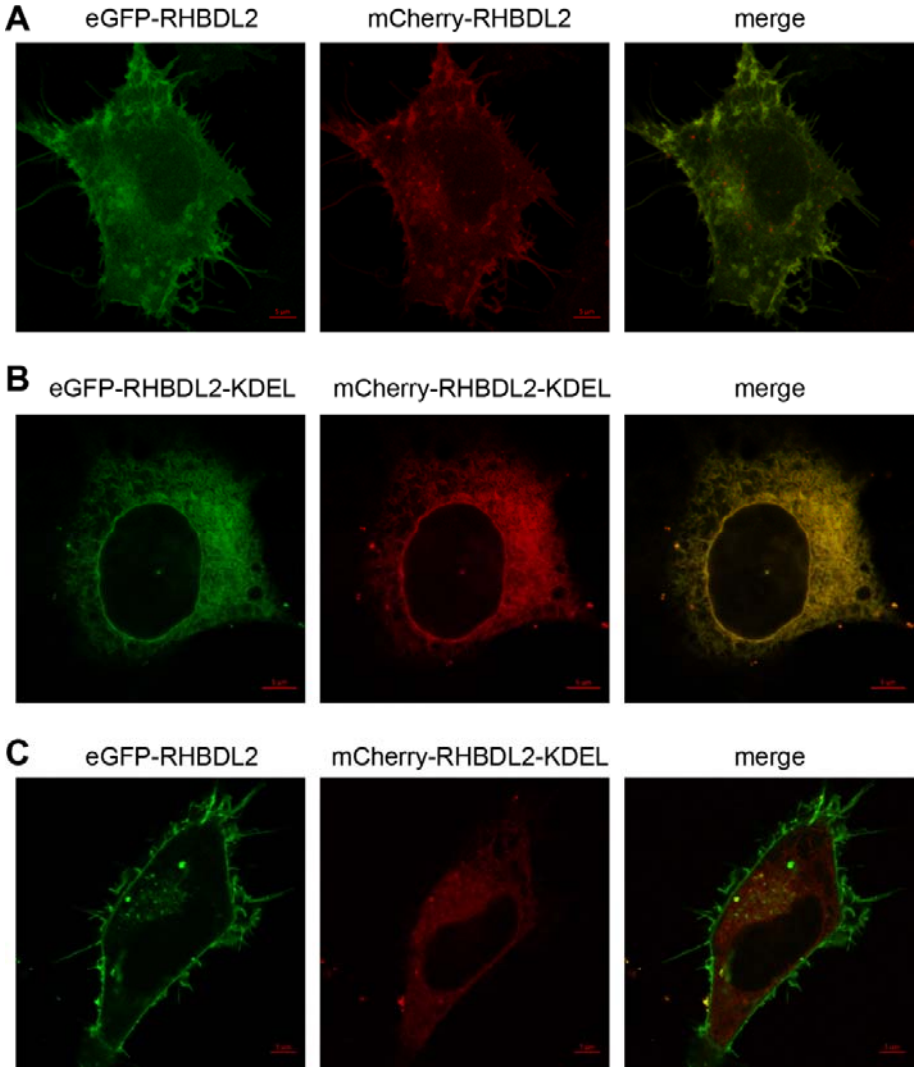

Table S1: Table of fitting parameters obtained in analysis of ACFs/CCFs reported in Fig. 1.

protein	ACF/CCF	*PN*/*A**	τ [ms]	*T*	t_0 [µs]
RHBDL2	ACF GFP	6.8	4.4	0.1	43
	ACF mCherry	8.7	7.3	0.6	114
GCPII	ACF GFP	0.9	4.2	0.2	23
	ACF mCherry	1.5	5.2	0.4	90
	CCF	0.2	6.4	0	NA
R2Ncyto control	ACF GFP	8.6	1.9	0.1	9
	ACF mCherry	10.3	1.9	0.4	74

**PN*/*A* holds for ACFs/CCFs.

ACFs were fited by a mathematical model accounting for lateral diffusion of a single type of fluorescent particles and for dark state transition (which is especially pronounced for mCherry tagged proteins):

$$G(t) = 1 + \frac{\left(1-T+T\cdot e^{-\frac{t}{t_0}}\right)}{1-T} \cdot \frac{1}{PN} \cdot \frac{1}{1+\frac{t}{\tau}}, \qquad (9)$$

where τ stays for the mean transition time, i.e. the time a molecule on average spends in the laser illuminated area, *PN* is the average number of fluorescent particles in the laser focus, *T* is the fraction of molecules that undergo the dark state transition, and t_0 represents the characteristic time of the transition.

CCFs were fit by the same model with zero fraction of the dark state transition. 1/*PN* represents the amplitude *A* of CCF.

Table S2: Surface concentrations of eGFP-/mCherry- labelled proteins used in our FCCS/FRET experiments.

Green color marks experiments where FCCS and FRET data were acquired. In all other cases, FRET only was acquired.

protein	1000*donor concetration	1000*acceptor concentration	FRET efficiency
	nm^{-2}	nm^{-2}	
R2Ncyto	0.18	0.05	0.07
	0.31	0.10	0.02
	0.33	0.44	0.03
	0.28	0.32	0.04
	0.21	0.34	0.05
	0.14	0.26	0.07
	0.16	0.48	0.06
	0.29	1.02	0.08
	0.18	0.93	0.09
	0.23	1.31	0.11
	0.13	1.26	0.10
	0.15	1.32	0.10
	0.16	1.34	0.12
	0.17	2.15	0.16
	0.09	2.59	0.21
	0.12	4.75	0.28
	0.07	2.24	0.19
	0.10	3.67	0.29
	0.06	3.65	0.25
	0.06	3.61	0.25
	0.06	4.77	0.29
RHBDL2	0.13	0.45	0.02
	0.10	0.21	0.05
	0.07	0.06	0.11
	0.09	0.25	0.02
	0.07	1.01	0.06
	0.10	1.29	0.08
	0.09	2.51	0.09
	0.10	3.32	0.14
	0.06	0.91	0.13
	0.09	0.25	0.02
	0.06	1.00	0.12
	0.07	1.68	0.08
	0.12	3.72	0.10
	0.09	2.24	0.07
GCPII	0.10	0.17	0.27

	0.06	0.13	0.30
	0.02	0.05	0.24
	0.04	0.05	0.27
	0.02	0.03	0.28
	0.02	0.08	0.27
	0.02	0.08	0.27
	0.01	0.05	0.33
	0.01	0.07	0.30